Geophys. J. R. astr. Soc. (1979) 58, 35–59

Phase velocity and *Q* of mantle Rayleigh waves

Ichiro Nakanishi * *Department of Earth Sciences, Nagoya University, Chikusa, Nagoya, Japan*

Received 1978 August 4; in original form 1978 February 3

Summary. We analysed the long-period Rayleigh waves that were generated by the Kurile Islands earthquake (1963), its largest aftershock, the Alaskan (1964) and the Tokachi-oki (1968) earthquakes. A deconvolution technique has been successfully applied to calculate the phase velocity and *Q*. We found significant regional differences in Rayleigh wave *Q*s which are closely correlated with regional variations in phase velocity and obtained pure-path phase velocities and *Q* for five tectonic provinces. The Rayleigh waves suffer small attenuation along the shield region where the phase velocity is high and large attenuation over the tectonically active regions where the phase velocity is low. Applying the *Q*-correction to the pure-path phase velocities the regional differences in phase velocity are considerably reduced. Studies of the frequency dependence of *Q* by the broad-band measurements of body waves are required in order to interpret correctly surface wave dispersion and free oscillation periods. Although the *Q* of the model MM8 (Anderson, Ben-Menahem & Archambeau) is appropriate as an average representation of the observed *Q* in the period range from 200 to 300 s, the differences for different great-circle paths are very large and the average *Q* values at periods below 200 s are lower than those of MM8.

1 Introduction

Since the occurrence of the great Chilean earthquake of 1960, a great deal of effort has been made to determine velocity and density profiles of the Earth by using the great-circle waves or normal modes and a spherical elastic model of the Earth has been well established. Less attention, however, has been paid to the determination of a *Q* model of the Earth, because the discrepancies among measurements of *Q* of seismic waves are too large. As shown by Payo (1969), Jackson & Anderson (1970) and Smith (1972) in their reviews of *Q* values and in more recent works of Wu (1972), Roult (1974, 1975), Jobert & Roult (1976), Mills & Hales (1977) and Sailor & Dziewonski (1978), measured surface wave and

* Present address: Earthquake Research Institute, University of Tokyo, Bunkyo-Ku, Tokyo, Japan.

free oscillation Qs vary a great deal. These variations may be accounted for by the following:

(1) As Reiter (1973) and Luh (1974) demonstrated by numerical experiments, lateral heterogeneities, which cause refraction, reflection and conversion of surface waves or splitting and coupling of normal modes, bias the determination of Q.
(2) Path coverage has not been sufficient to obtain the average Q versus T (period) curve.
(3) The measurement of amplitude of a particular normal mode is disturbed by the superposition of other modes. Roult (1974, 1975) and Jobert & Roult (1976) greatly reduced the effects caused by mode superposition through the use of a time-variable filtering technique (Cara 1973).

Recently, Akopyan, Zharkov & Lyubimov (1975, 1976), Randall (1976), Liu, Anderson & Kanamori (1976) and Kanamori & Anderson (1977) have revived the dispersion-attenuation relation stressed by Futterman (1962), Jeffreys (1965, 1975) and Carpenter & Davies (1966) and demonstrated that the fractional change in phase velocity due to Q is proportional to Q^{-1} and the uncertainty of Q of seismic waves limits knowledge of the velocity structure of the Earth. Because this effect of attenuation on phase velocity of surface waves is larger than the standard deviations of observed great-circle phase velocities, we have to take into account a regionality of the observed Q in order to interpret correctly a regional difference in the observed phase velocities. The studies of lateral heterogeneities by the great-circle waves (Toksöz & Anderson 1966; Kanamori 1970a; Dziewonski 1971a; Wu 1972; Okal 1977), however, have used only the phase or group velocities and discussed the regional differences in velocity structure without taking into account the regionality in Q.

The purpose of the present study is:

(1) to obtain an average $Q(T)$ curve of Rayleigh waves accurate enough to determine an average Q model of the upper mantle of the Earth and
(2) to investigate regional differences in phase velocity and Q and the relation between them.

2 Data

We analysed 64 pairs of Rayleigh waves recorded on the long-period vertical seismograms from the stations of the World Wide Standard Seismograph Network (WWSSN). We used three great earthquakes and one large aftershock. Pertinent data concerning these earthquakes are listed in Table 1. Lists of the stations and phases used are presented in Table 2. Locations of the earthquakes and stations are shown in Fig. 1. It is apparent that the path coverage of the present study is more complete than those of any previous studies. The path coverage is dependent on the radiation pattern of the earthquake. The following gives the detailed descriptions of the records of each earthquake.

Table 1. List of earthquakes used.

Locations	Latitude	Longitude	Date	Time	Depth (km)	Magnitude
Kurile Islands	44.8° N	149.5° E	1963 October 13	05 17 57	60	8.3
Kurile Islands	44.9° N	150.3° E	1963 October 20	00 53 11	26	7.0
Alaska	61.0° N	147.8° W	1964 March 28	03 36 14	33	8.5
Tokachi-oki	40.8° N	143.2° E	1968 May 16	00 48 55	7	8.0

Table 2. Pertinent data concerning the stations, phases used, lengths of great-circle paths and percentages of great-circle paths lying in each of the five regions.

Kurile Islands earthquake of 1963 October 13

Station code	Δ deg	L km	Phases	ℓ_S	ℓ_M	ℓ_T	ℓ_R	ℓ_O
AAE	98.0	40038.7	R3, R4, R5, R6	15.4	29.3	2.9	8.1	44.3
AAM	81.0	40021.2	R3, R5	25.4	20.7	11.7	1.9	40.3
ADE	80.2	40010.0	R4, R6	24.7	12.9	8.4	10.6	43.4
AFI	68.3	40023.7	R3, R5	17.1	0.0	11.1	10.4	61.4
ATU	84.0	40023.1	R4, R6	23.6	7.0	13.4	6.6	49.4
BEC	97.0	40016.9	R3, R7	20.5	12.4	16.1	1.4	49.6
BUL	125.7	40042.9	R4, R6	13.1	24.5	3.8	19.7	38.9
COP	73.4	40014.5	R5, R7	33.9	4.9	16.2	2.4	42.5
GDH	64.8	40009.9	R3, R5, R7	28.1	11.8	12.1	6.4	41.6
GEO	86.6	40019.9	R3, R5	22.2	18.1	12.7	1.4	45.6
HNR	54.9	40010.8	R4, R6	16.0	3.0	20.1	6.4	54.5
IST	79.1	40023.9	R3, R4, R5, R6	22.9	8.2	12.1	7.0	49.7
KON	70.7	40013.1	R5, R7	34.3	5.4	18.9	2.2	39.2
LAH	58.5	40040.7	R4, R6	15.2	27.6	3.2	15.5	38.7
MDS	77.4	40022.9	R3, R5	26.7	24.6	11.8	3.0	33.9
NAI	106.8	40040.8	R4, R6	15.6	27.9	3.2	14.9	38.5
NDI	58.2	40041.9	R4, R6	13.0	27.4	3.5	18.9	37.1
PDA	97.5	40009.3	R3, R7	13.9	7.0	16.7	8.5	53.9
PRE	129.6	40043.3	R4, R6	10.9	18.6	6.4	20.2	43.9
QUE	64.4	40039.7	R4, R6	15.8	28.5	3.1	12.0	40.7
RAB	48.9	40009.3	R2, R4	16.8	2.8	22.6	7.0	50.8
SHI	73.9	40036.4	R4, R6	12.5	28.3	4.3	4.9	50.1
TAU	87.5	40009.2	R2, R4	22.2	15.3	9.8	12.6	40.1
TOL	92.2	40013.1	R5, R7	34.2	5.4	19.1	2.0	39.3

Kurile Islands earthquake of 1963 October 20

Station code	Δ deg	L km	Phases	ℓ_S	ℓ_M	ℓ_T	ℓ_R	ℓ_O
ARE	135.0	40037.1	R1, R3	4.5	14.8	15.1	25.0	40.6
BKS	62.8	40035.6	R2, R4	6.6	15.4	15.5	22.9	39.6
FLO	80.3	40025.1	R2, R4	24.7	25.4	15.2	6.4	28.2
HNR	54.9	40010.5	R2, R4	15.8	3.0	19.1	6.5	55.7
IST	79.5	40023.6	R2, R4	23.2	8.0	11.8	6.8	50.2
KEV	58.3	40013.0	R2, R4	34.9	5.5	18.2	2.2	39.2
MAL	95.4	40013.1	R2, R4	35.0	5.5	18.0	2.3	39.2
MDS	77.0	40023.2	R2, R4	26.4	24.4	12.0	3.3	34.0
PTO	92.1	40011.6	R2, R4	31.2	6.2	21.7	0.0	40.9
QUE	64.9	40039.5	R3, R5	15.7	28.8	2.9	11.9	40.7
SHA	87.8	40027.3	R2, R4	23.2	23.1	16.0	12.2	25.4
STU	80.6	40015.0	R2, R4	33.1	4.9	15.0	1.8	45.3

Alaskan earthquake of 1964 March 28

Station code	Δ deg	L km	Phases	ℓ_S	ℓ_M	ℓ_T	ℓ_R	ℓ_O
ADE	112.7	40020.7	R3, R5	24.0	3.7	12.6	11.6	48.1
ANP	68.6	40024.1	R5, R7	13.4	22.6	12.9	9.2	41.0
BAG	76.5	40024.6	R5, R7	18.0	16.1	17.7	7.7	40.5
HKC	74.5	40023.5	R4, R6	5.6	26.0	12.1	11.1	45.1
MAN	77.8	40024.7	R5, R7	18.0	13.8	20.2	7.2	40.8
MUN	119.6	40024.5	R3, R5	20.1	2.3	16.2	7.2	54.2
RAB	79.7	40021.5	R5, R7	22.1	4.1	11.1	11.2	51.5

Tokachi-oki earthquake of 1968 May 16

Station code	Δ deg	L km	Phases	ℓ_S	ℓ_M	ℓ_T	ℓ_R	ℓ_O
AFI	68.7	40030.2	R3, R5	16.5	0.0	11.7	7.1	64.7
ANP	23.9	40035.5	R3, R5	19.3	10.9	10.5	17.4	42.0
HKC	30.7	40039.1	R2, R4	10.5	11.4	13.5	27.4	37.3
LPB	143.7	40036.8	R3, R4, R5, R6	8.3	13.6	16.6	21.9	39.5
MAL	97.1	40016.3	R3, R5	27.1	5.0	22.4	2.3	43.2
MSH	63.0	40040.1	R3, R5	8.4	25.5	4.7	5.4	56.1
NAI	103.2	40046.7	R4, R6	14.0	24.5	4.9	16.0	40.6
NDI	54.3	40046.6	R4, R6	13.9	24.4	5.0	16.7	40.2
NNA	134.6	40039.6	R3, R4, R5, R6	2.8	11.8	15.0	28.0	42.5
NUR	67.1	40017.5	R3, R5	24.6	5.2	19.0	1.2	50.0
POO	62.6	40047.7	R4, R6	12.4	22.2	5.2	19.6	40.6
PRE	124.8	40047.5	R4, R6	6.9	19.3	5.5	17.9	50.4
RAB	45.7	40011.0	R2, R4	20.7	3.0	24.8	7.3	44.2
SHL	44.9	40047.5	R4, R6	9.3	20.1	5.4	18.3	46.8
SNG	50.6	40038.4	R3, R5	12.6	11.3	12.7	25.2	38.3

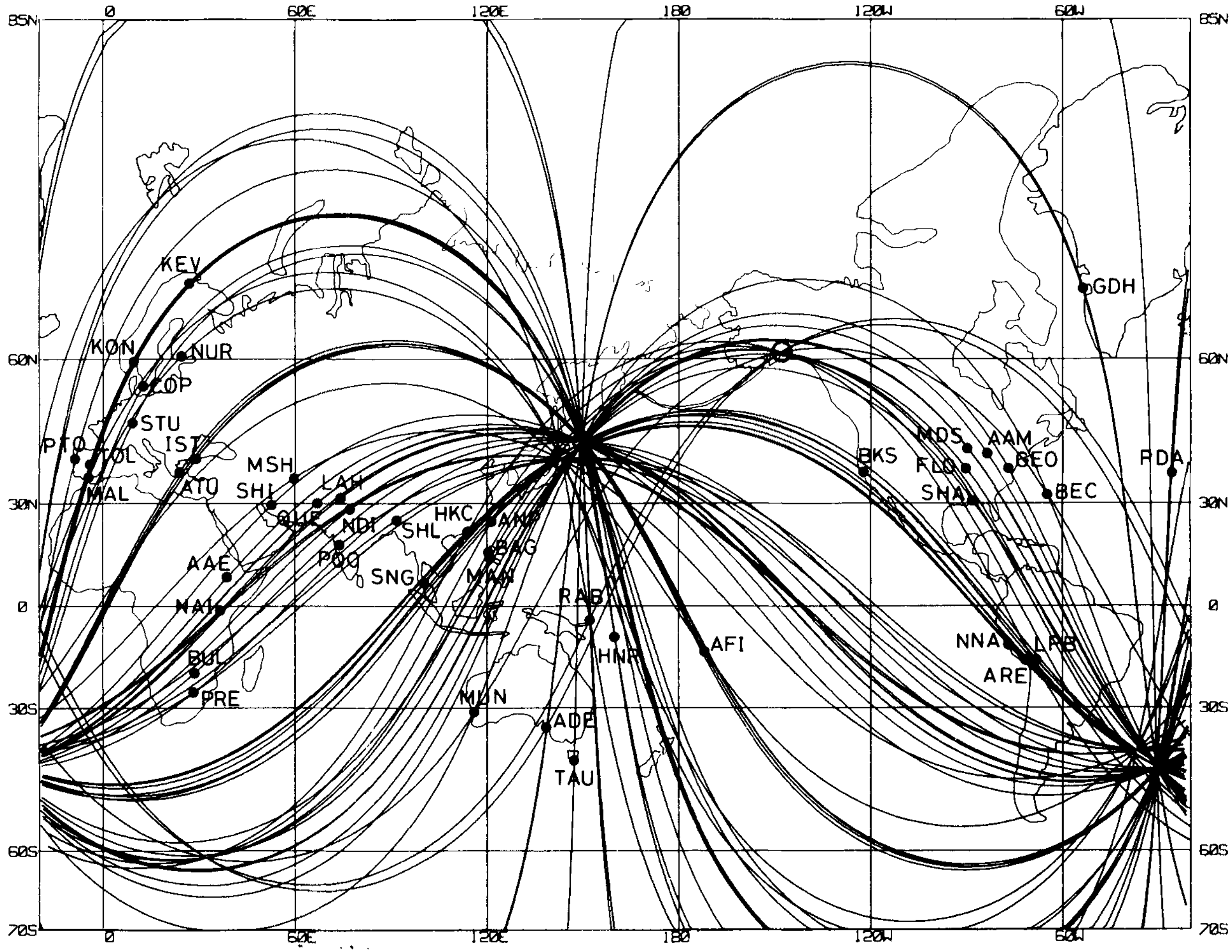

Figure 1. Station locations and great-circle paths over which phase velocity and Q of mantle Rayleigh waves are available. The sources are indicated by open circles. As the epicentre of the Kurile Islands earthquake is very close to that of its aftershock, the locations of both shocks can not be discriminated. Solid circles indicate the station locations.

2.1 KURILE ISLANDS EARTHQUAKE

We obtained about one-half of all data from the Kurile Islands earthquake of 1963 October 13 (see Table 2). Since Q of surface waves is strongly dependent on the tectonic characteristics of the path, the path coverage should be as uniform as possible, in order to obtain reliable global average of the Q values of surface waves. The path coverage, however, is limited by the radiation pattern of the earthquake used. Since the direction of a nodal line of the Kurile Islands earthquake is about N40° E, surface waves with large amplitude were not observed at stations in North and South America (Kanamori 1970b). Although nine records from the stations in this direction were used in a preliminary report of this study (window 3 in fig. 1 of Nakanishi 1978a, b), these records are poorest in quality of all the data and are excluded from the present study. The magnitude of this earthquake (surface-wave magnitude = 8.3) is appropriate for the study on the velocity and attenuation of mantle waves.

2.2 AFTERSHOCK OF THE KURILE ISLANDS EARTHQUAKE

The largest aftershock of the Kurile Islands earthquake occurred on 1963 October 20. This aftershock generated Rayleigh waves which do not contain high-frequency components in the spectrum. Therefore, the low-frequency wavelets of Rayleigh waves are clearly seen on the records and the quality of the records is very good. The normalized mean square errors of Wiener filter are very small in all cases (see the next section). We analysed this aftershock in order to determine the phase velocity and Q in the period range between 100 and 250 s, especially at periods below 200 s.

2.3 ALASKAN EARTHQUAKE

This earthquake is the largest of all earthquakes which have occurred after the installation of the WWSSN stations. The surface-wave magnitude of the Alaskan earthquake is 8.5, too large to study the surface waves at periods below 300 s. Dziewonski & Gilbert (1972) and Dziewonski, Mills & Bloch (1972) studied the eigenperiods and dispersion of the free oscillations generated by the Alaskan earthquake using the records from the WWSSN stations but they did not investigate the attenuation of the free oscillations. For the Alaskan earthquake, the paths studied here cover the regions where the phase velocities and Q are high.

2.4 TOKACHI-OKI EARTHQUAKE

The source mechanism of the Tokachi-oki earthquake was studied by Kanamori (1971). Because the WWSSN instruments had their frequency characteristics changed to 15–100s ($T_0 - T_g$) around 1966, the response at 200–300 s was much curtailed at the time of occurrence of the Tokachi-oki earthquake. Therefore, the magnitude of this earthquake is a little too small to study Rayleigh waves at periods between 200 and 300 s.

3 Methods of analysis

The vertical component seismograms were digitized at an interval of about 4 s. The digitized records were detrended, low-pass filtered and resampled at an interval of about 8 s. We determined the great-circle phase velocities and Q from multiple Rayleigh waves.

The successive Rayleigh waves along a great-circle path can be formulated as

$$R_{2n+1} = W * R_{2n-1}$$

or

$$R_{2n+2} = W * R_{2n} \qquad n = 1, 2, \ldots \tag{1}$$

where W is the unknown transfer function of one circling around the Earth, R_i is Rayleigh wave of order i, and $*$ indicates convolution. We estimated the optimum W using the Wiener filtering technique (Wiener 1949). This technique has been used in the deconvolution of reflection seismograms and recently applied to the estimation of spectral ratio of two time series (Saito 1976; Kikuchi 1977). Principles of the digital Wiener filter are discussed by Robinson & Treitel (1967). We describe here only the essence of Saito's method.

For brevity, we replace R_{2n-1} and R_{2n+1} with X_t and Y_t, respectively. Equation (1) can be written as

$$Y_t = \sum_{\tau=-\infty}^{\infty} W_\tau \cdot X_{t-\tau}. \tag{2}$$

If we obtain the transfer function W_t, the corresponding output is expressed as

$$\hat{Y}_t = \sum_{\tau=0}^{M} W_\tau \cdot X_{t-\tau}, \tag{3}$$

where M is the length of the transfer function W_t.

A transfer function which satisfies

$$E[\,|Y_t - \hat{Y}_t|^2] = \min \tag{4a}$$

is optimum in Wiener's sense, where E indicates the expected value symbol. Claerbout & Robinson (1964) and Robinson & Treitel (1967) have shown that the performance of a filter with fixed length can be considerably improved by delaying the output Y_t with respect to the input X_t. If we delay the desired output Y_t by τ_1, equation (4a) is rewritten as

$$E\left[\left|Y_{t-\tau_1} - \sum_{\tau=0}^{M} W_\tau \cdot X_{t-\tau}\right|^2\right] = \min. \tag{4b}$$

By the usual technique used in the least-squares analysis, equation (4b) leads to the well-known normal equation

$$\sum_{\tau=0}^{M} W_\tau \cdot \Phi_{xx}(t-\tau) = \Phi_{yx}(t-\tau_1); \qquad t = 0, 1, \ldots, M \tag{5}$$

where

$$\Phi_{xx}(t-\tau) = E[X_{j+t-\tau} \cdot X_j] = E[X_{j-\tau} \cdot X_{j-t}]$$

and

$$\Phi_{yx}(t-\tau_1) = E[Y_{j+t-\tau_1} \cdot X_j].$$

If equation (5) is solved, the mean square error of the transfer function W_t can be obtained by the formula

$$e_{\mathrm{rms}}^2 = \Phi_{yy}(0) - \sum_{\tau=0}^{M} W_\tau \cdot \Phi_{yx}(\tau - \tau_1), \tag{6}$$

where

$$\Phi_{yy}(0) = E\,[Y^2_{t-\tau_1}].$$

Thus, if the filter length M and the lag τ_1 are given, the optimum transfer function W_t is determined solving equation (5) by Levinson's (1947) and Simpson's algorithm (Wiggins & Robinson 1965). Therefore, we must determine the optimum filter length M and lag τ_1. Saito (1976) has proposed a criterion. This criterion states that the filter length M and lag τ_1 which satisfy the following equation (7) are optimum:

$$\hat{e}^2_{\text{rms}} = \frac{e^2_{\text{rms}}}{N - (M+1)} = \min, \tag{7}$$

where N is the length of X_t and Y_t.

We determined the optimum transfer function W_t using the above-mentioned procedure. If we obtain the transfer function W_t, we can easily calculate the great-circle phase velocity and Q through the Fourier transformation of W_t. Slightly modifying equation (1) of Kanamori (1970a), we obtain the formula for the great-circle phase velocity:

$$C = \frac{L}{(t_{n+2} - t_n - \Delta t \cdot \tau_1) + T \cdot [\Phi_w(\omega)/2\pi + N + ½]} \tag{8}$$

where L is the length of the great-circle path, t_i the starting time of the record of the surface wave of order i, Δt the sampling interval, τ_1 the optimum lag, T the period, $\omega = 2\pi/T$, $\Phi_W(\omega)$ the phase spectrum of the optimum W_t, N an integer and the factor ½ comes from the polar phase shifts. The integer N is fixed so that the phase velocity at long-period can connect smoothly with the free oscillation data. Although Dahlen (1975) suggested that the apparent length of a great-circle path applicable to measurements of phase velocities of mantle waves is sensitive to the details of the lateral heterogeneities in the mantle, Dziewonski & Sailor (1976) and Dahlen (1976) showed that this result was in error and that the correction for the apparent path length is negligible in comparison with the present level of accuracy in great-circle phase velocity measurements. Therefore, we use the length of the geodesic once around the geoellipsoid (Maruyama 1967) as L.

The formula for Q is, according to Kanamori (1970a):

$$Q = \frac{\pi \cdot [(t_{n+2} - t_n - \Delta t \cdot \tau_1) + (d/d\omega)\Phi_W(\omega)]}{-T \cdot \ln\,[A_W(\omega)]} \tag{9}$$

where $A_W(\omega)$ is the Fourier amplitude of the optimum W_t. We calculated $d\Phi_W(\omega)/d\omega$, interpolating the phase spectrum $\Phi_W(\omega)$ by the cubic splines. The coefficients of the cubic splines were determined by the algorithm described by Pennington (1965). The Q values obtained by equation (9) were averaged over 0.0006 cps overlapping windows. If the obtained transfer function W_t is processed with the moving window technique (Dziewonski, Bloch & Landisman 1969), we can easily determine the great-circle or inter-station group velocity.

As an example of the Wiener filtering, we present the results from the Kurile Islands earthquake of 1963 October 13 recorded at AAE. The original records used in the analysis are shown in Fig. 2(a). In this example, the seismograms are group velocity windowed with fixed group velocities of 3.45 and 4.1 km/s. The logarithm of the normalized mean square errors for R3–R5 pair at AAE are plotted against the filter length M in Fig. 2(b). We searched for the optimum lag, at which $\hat{e}^2_{\text{rms}}$ has a minimum value, for each filter length

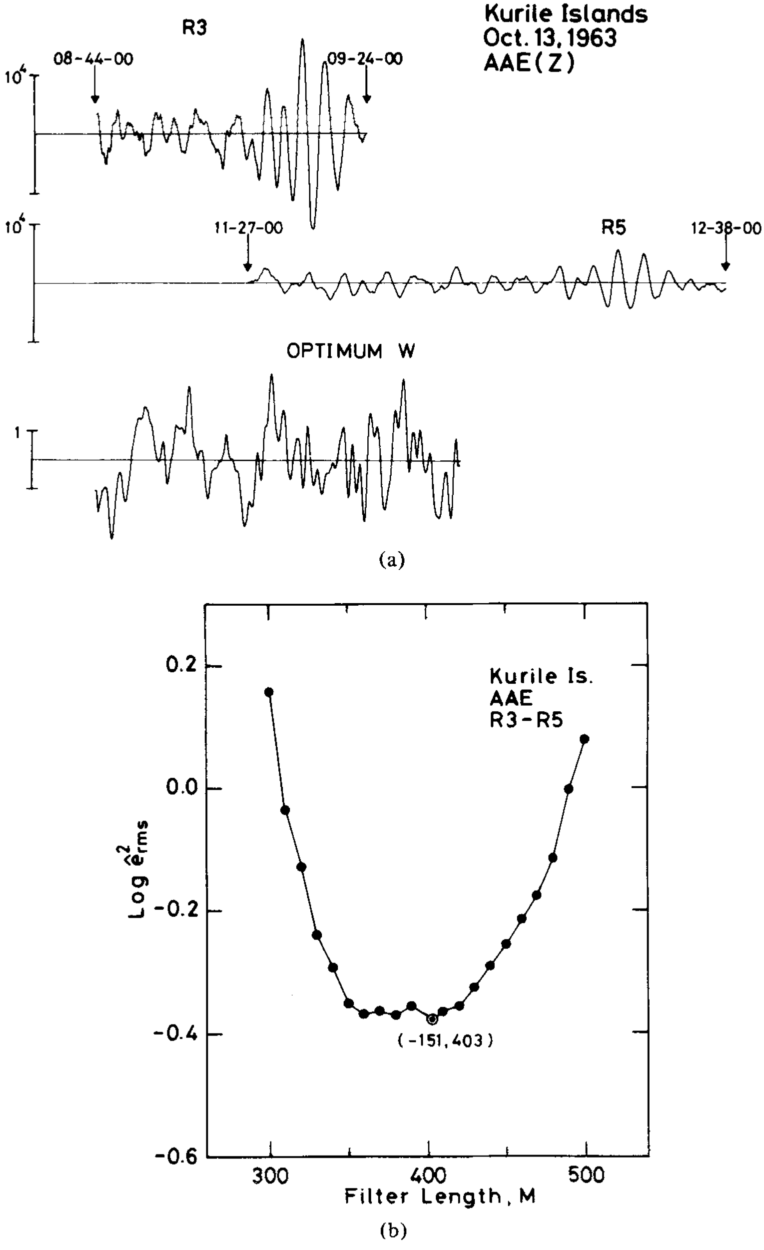

Figure 2. Example of Wiener filtering. R3–R5 pair of the Kurile Islands earthquake recorded at AAE is used. (a) Original traces of R3 and R5 and optimum transfer function W. The vertical scale is arbitrary. (b) Log $\hat{e}^2_{rms}$ versus M (filter length) curve. The optimum delay and filter length are 151 and 403, respectively. (c) Phase velocity and Q. The difference of the phase velocity from the value for the 5.08M model (Kanamori 1970a) is shown. Kanamori's (1970a) results are indicated by open circles.

using the Simpson's algorithm (Wiggins & Robinson 1965). The normalized mean square error is shown for each filter length in Fig. 2(b). $(-\tau_1, M)$ indicates the optimum lag τ_1 and the optimum length M, at which $\hat{e}^2_{rms}$ has a minimum value. The optimum transfer function is shown in the bottom of Fig. 2(a). The optimum lag and filter lengths for R3–R5

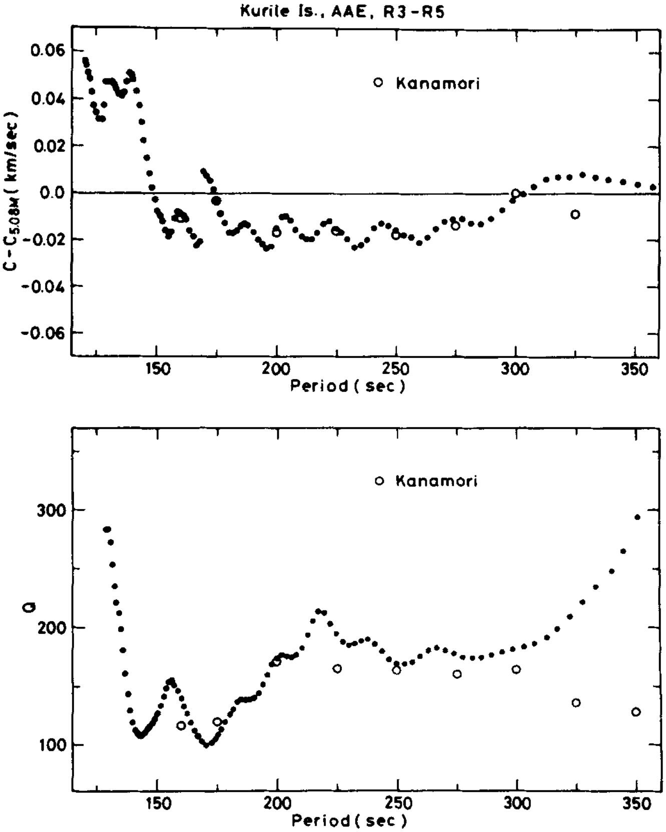

Figure 2 (c)

pair of AAE are 151 and 403 digits, respectively. The digital interval is 8.11 s. In this case, the performance of the criterion is good. The values of the optimum lag and filter length seem to be reasonable, because $(M - \tau_1) = 252$ digits are nearly equal to the length which corresponds to the group velocity window of 3.45 and 4.1 km/s. We then calculated the Fourier transformation of the optimum W_t and obtained the phase velocity and Q which are plotted in Fig. 2(c). Also in Fig. 2(c) are plotted the results obtained by Kanamori (1970a) from the same record. It is apparent that our results at periods between 160 and 300 s are in good agreement with those of Kanamori who used the conventional Fourier transformation method to estimate the spectral difference between R3 and R5.

4 Results

Before discussing the detailed results of the present study some mention should be made of the precision of the measurements of phase velocity and Q. We use the R5–R7 pairs of the Kurile Islands earthquake recorded at KON ($\Delta = 70.7°$) and TOL ($\Delta = 92.2°$) in Fig. 3 for this purpose. Azimuths from the epicentre to KON and TOL are 339.77° and 340.01°, respectively. The difference between the azimuths of the two stations is very small. The agreement of the phase velocities observed at KON and TOL in the period range from 180 to 300 s is remarkable. The difference between the Q values obtained for KON and TOL, however, is much larger than that of the phase velocities. The quality of both the records is

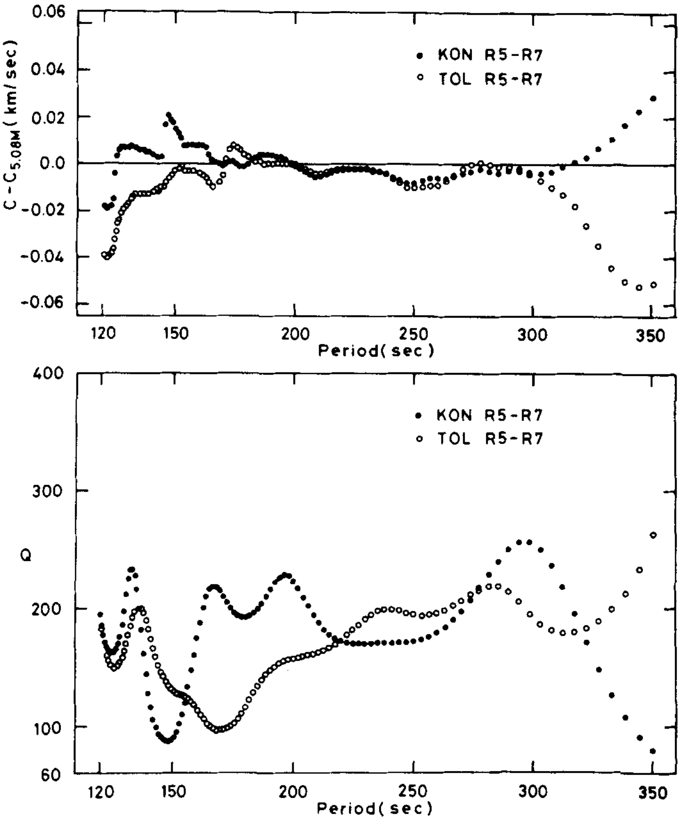

Figure 3. Phase velocity and Q obtained for different stations which stand at almost the same great-circle path. These figures give a rough estimate of the precision of the measurements of phase velocity and Q. R5–R7 pairs from the Kurile Islands earthquake recorded at KON and TOL are used for this purpose. Azimuths from the epicentre to KON and TOL are 339.77° and 340.01°, respectively. The difference of the phase velocity from the value for the model 5.08M is shown.

very good. Therefore, even if the quality of data is good, we have to expect a relatively large uncertainty in the observed Q.

We analysed 64 pairs of Rayleigh waves and calculated the average phase velocities and Q values in the period range from 100 to 333.33 s. We describe the overall characteristics of these average values and compare them with the results of the previous authors. Detailed tabulations of the values of phase velocity and Q for individual records used here are presented in Nakanishi (1978a).

PHASE VELOCITY

The average phase velocity is presented in Table 3 and Fig. 4(a). The figure shows the difference of the phase velocity from the value for the 5.08M earth model (Kanamori 1970a). This model has been currently used to synthesize the long-period surface waves for the investigation of source mechanisms after the famous study by Kanamori (1970b, c, 1971). The 5.08M model was originally constructed so that it fitted the group velocity of both Rayleigh and Love waves (Kanamori 1970a). The phase velocity for this model is in

Table 3. Averages and standard deviations of phase velocities and Q of Rayleigh waves.

T sec	C km/sec	σC km/sec	Q	σQ	No. of obs.
333.33	5.5326	0.0141	143	69	33
312.50	5.3859	0.0078	189	68	34
294.12	5.2514	0.0068	231	61	34
277.78	5.1292	0.0078	215	47	52
263.16	5.0201	0.0078	196	38	52
250.00	4.9211	0.0124	184	36	64
238.10	4.8344	0.0146	182	37	64
227.27	4.7601	0.0146	180	37	64
217.39	4.6923	0.0166	174	33	64
208.33	4.6310	0.0141	169	31	64
200.00	4.5781	0.0130	166	32	64
192.31	4.5312	0.0130	159	35	63
185.19	4.4889	0.0110	148	35	62
178.57	4.4510	0.0124	138	33	59
172.41	4.4177	0.0078	131	30	53
166.67	4.3883	0.0103	126	29	53
161.29	4.3609	0.0130	121	28	53
156.25	4.3370	0.0141	119	29	53
151.52	4.3154	0.0146	120	31	51
147.06	4.2948	0.0175	121	29	47
142.86	4.2748	0.0187	127	32	42
138.89	4.2579	0.0187	131	36	42
135.14	4.2416	0.0191	130	37	41
131.58	4.2251	0.0195	128	39	40
128.21	4.2106	0.0207	128	39	38
125.00	4.1973	0.0217	132	48	35
121.95	4.1839	0.0244	133	52	35
119.05	4.1735	0.0290	138	56	35
116.28	4.1646	0.0103	115	30	9
113.64	4.1541	0.0110	119	23	9
111.11	4.1437	0.0124	120	14	9
108.70	4.1329	0.0156	124	6	8
106.38	4.1240	0.0179	130	11	8
104.17	4.1165	0.0179	132	18	8
102.04	4.1085	0.0170	131	20	8
100.00	4.0986	0.0151	131	20	8

good agreement with the oceanic phase velocity of both Rayleigh and Love waves in the period range between 150 and 300 s (Kanamori 1970a). The average of the observed phase velocities obtained here is lower than that of the model 5.08M, the velocity difference being about 0.005 km/s in the period range from 180 to 300 s. We obtained a much lower average phase velocity than that of the model 5.08M at 100 s, the velocity difference being about 0.025 km/s. Although the standard deviation is somewhat oscillating, it has a value of about 0.012 km/s in the period range between 150 and 300 s.

Extensive studies on phase velocity of Rayleigh waves have been made by Kanamori (1970a), Dziewonski (1971a), Dziewonski *et al.* (1972) and Wu (1972). The comparison of our results with two of these authors is made in Fig. 4(a). Several characteristics of each result are apparent in the figure. We obtained higher phase velocities at periods above 200 s than those of the other two studies. We obtained slightly higher phase velocities than Kanamori (1970a). This may be due to the fact that the present study includes more data from paths through the shield regions than Kanamori's. Dziewonski (1971a) and Dziewonski *et al.* (1972) analysed the Peru–Bolivian border and the Alaskan earthquake, respectively. The agreement between the results of the two studies is surprisingly good. Wu (1972) obtained the lowest phase velocities of all these authors from the Rat Island earthquake of 1965 February 4. This earthquake, however, has a strong aftershock which interferes with the R7 phase of the main shock and Wu used many R5–R7 pairs from this earthquake in order to obtain the phase velocity and Q. This interference between the R7 phase and aftershock must result in uncertainty in Wu's phase velocity. There is one additional reason for us not to regard his phase velocity as an average representation of the observed ones. Wu & Kanamori (1973) studied the source mechanism of the Rat Island earthquake and showed that this earthquake has a dipolar Rayleigh wave radiation pattern. The records from the stations in North and South America and Asia cannot be used because of this radiation

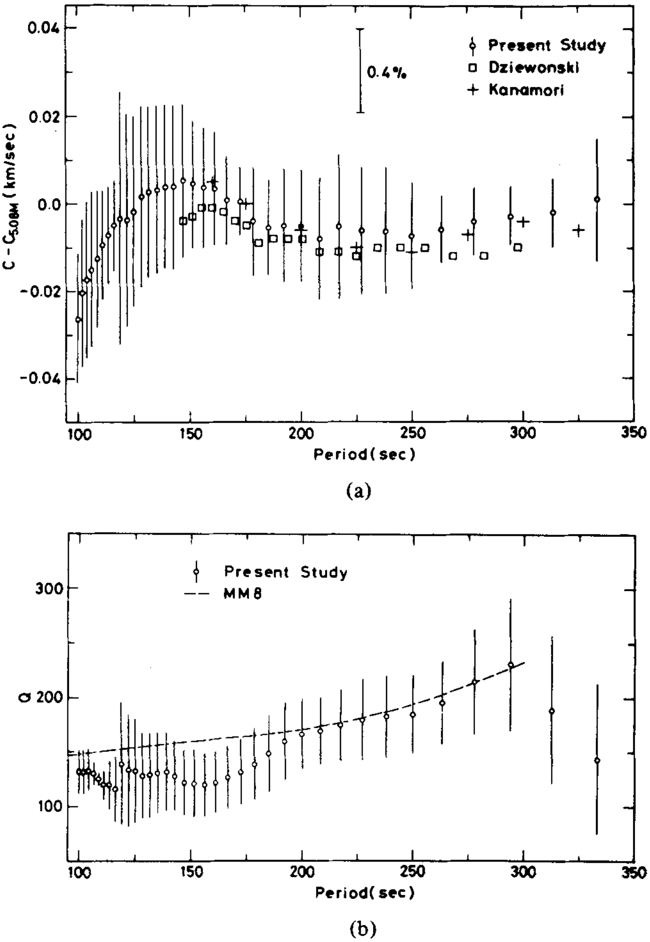

Figure 4. Average phase velocity and Q of mantle Rayleigh waves. (a) Average and standard deviation of phase velocities. The difference of the phase velocity from the value for the model 5.08M is shown. Kanamori's (1970a) and Dziewonski's (1971a) results are indicated by crosses and squares, respectively. (b) Average and standard deviation of Q. Value of Q calculated for MM8 (Anderson *et al.* 1965, fig. 5) is shown for comparison. (c) Comparison of our Q values with those of the previous authors: Sailor & Dziewonski (1978, table 2); Jobert & Roult (1976, table 5) or Deschamps (1977, table 1); Abe *et al.* (1970, fig. 9); Kanamori (1970a, table 9); MM8 (Anderson *et al.* 1965, fig. 5). Also indicated are the standard deviations of our Q values at periods 100.0, 151.52, 200.0, 250.0 and 294.12 s.

pattern. The narrow path coverage due to the dipolar radiation pattern may result in some bias in the average phase velocity.

Q

The average Q values are presented in Table 3 and Fig. 4(b, c). It is apparent in the figure that Q of Rayleigh waves has a minimum value of about 120 at 150 s and increases to a value of about 230 s at 300 s. Fig. 4(b) makes the comparison of our average Q with the theoretical one for the model MM8 of Anderson, Ben-Menahem & Archambeau (1965). Two important features can be seen in the figure. First, although Q of MM8 is appropriate

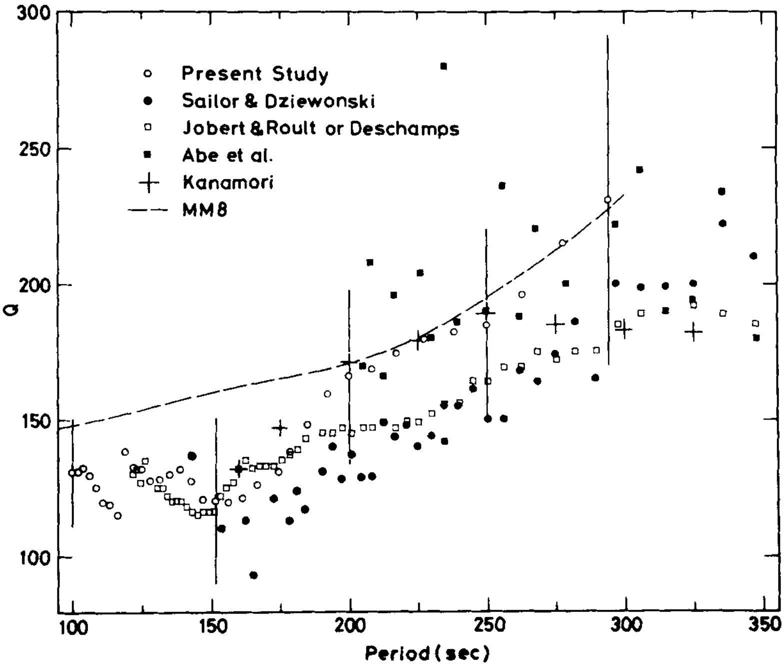

Figure 4 (c)

as a representation of the observed Q in the period range from 200 to 300 s, the standard deviation is large (about 40 in this period range). Secondly, our average Q is lower than that of MM8 at periods below 200 s. The latter indicates that the low-Q zone, which may be identical with the low-velocity zone in the upper mantle, must be more extensive than that of the model MM8. In the following, our results are compared with those of previous authors.

Since the pioneering and extensive work by Ben-Menahem (1965), the attenuation of mantle waves has been studied by a number of investigators such as Kanamori (1970a), Abe, Sato & Frez (1970), Wu (1972), Jobert & Roult (1976), Mills & Hales (1977) and Sailor & Dziewonski (1978). There are, however, significant discrepancies among these studies. The large scatter in the available Q-data of surface waves and free oscillations has discouraged us from inversion attempts for an anelastic structure of the Earth. The inversion of the Q-model has not yet seriously been attempted since Anderson *et al.* (1965) derived the Q-model MM8. The comparison of our results with those of the previous studies is made in Fig. 4(c). It is apparent that there is a large scatter in the results of all the studies. In particular, there are large differences between the results of the present, Jobert & Roult's (1976) and Sailor & Dziewonski's (1978) studies. The Q values obtained by the latter two authors are systematically lower than those obtained by us. The difference is about 30 throughout the period range between 200 and 300 s. Our and Jobert & Roult's Q values agree well at periods below 180 s. Jobert & Roult determined Q from the temporal decrease in amplitude of the free oscillations. The lower values obtained by them must be due to the narrow azimuthal coverage of their study and the strong dependence of Q values of seismic waves on the tectonic nature of the path. Jobert & Roult analysed earthquakes that occurred along the circum-Pacific tectonic belt and were recorded at the stations in France. Their Q values must have some bias due to the narrow azimuthal coverage, the long path along such tectonically active regions as the East Pacific Rise, the Red Sea, the Himalayas and the short path over such regions as the Brazilian and Siberian shields. These are apparent in fig. 3 of Jobert & Roult (1976) and in Fig. 7 of this paper. The large attenuation along the tectonically active regions will be shown in the next section. Sailor & Dziewonski's (1978) values of Q are the lowest of all the studies. They determined Q of free oscillations by stacking numerous WWSSN records of two deep earthquakes and fitting a resonance curve to the spectral stack. The Q values determined by this method, however, may be biased by broadening of the spectral peaks due to the rotation, ellipticity and lateral heterogeneities of the Earth. The error due to the lateral elastic heterogeneities of the real Earth has not been estimated, because we have not much information about the lateral heterogeneities and because the theoretical treatment for lateral heterogeneities has not been developed. Abe *et al.* (1970) studied the free oscillations from the Kurile Islands earthquake of 1963 October 13 and determined the Q values in the period range between 200 and 480 s by the time-decay of spectral peaks. Although a large scatter exists in their Q values, they are on the whole in agreement with our Q values. The azimuthal coverage of Abe *et al.*'s study is relatively complete. Mills & Hales have recently studied Q of Rayleigh waves from the Kurile Islands earthquake of 1963 October 13 but did not tabulate the Q-values in their paper.

5 Regionality in phase velocity and Q

5.1 A BRIEF REVIEW OF THE STUDIES ON REGIONALITY IN DISPERSION OF SURFACE WAVES

Inversion of lateral heterogeneities in the deep mantle was first attempted by Toksöz & Anderson (1966) who derived the pure-path phase velocities for such regions as oceanic, tectonic and shield by use of great-circle Love waves. The basic assumption of their study is that the overall phase delay of a surface wave is a linear function of the individual phase delays over the various segments of the paths. Although Toksöz & Anderson used a small number of observations (six observations) in order to solve a system of linear equations of three unknowns by a least-squares method, they obtained a reasonable conclusion that the pure shield and tectonic paths have the highest and lowest phase velocities, respectively, in the period range between 100 and 300 s. A theoretical basis for the inverse problem in the context of the geometrical optics approximation has been given by Backus (1964). The distribution of the paths over the Earth was not dense enough, nor uniform enough, for Toksöz & Anderson to apply Backus's theory to the interpretation of the observations. Kanamori (1970a) obtained pure-path phase velocities for both Love and Rayleigh waves using the same procedure as Toksöz & Anderson (1966) and determined the shear wave velocity structures for oceanic and tectonic regions. Dziewonski (1971a, b) derived the pure-path phase and group velocities for Rayleigh waves from a number of observations and determined the regionalized upper mantle models. Dziewonski (1971b) obtained an important conclusion that the regional differences in phase velocity may be explained by models with the significant velocity contrasts confined above 200 km. Both Kanamori (1970a) and Dziewonski (1971a) used plate V of Umbgrove (1947) in order to regionalize the Earth's surface. Wu (1972) studied Rayleigh waves generated by the Rat Island earthquake and derived the pure-path phase velocities for such regions as ocean, continent (or shield), arc and ridge. His regionalization is based on the new global tectonics. Recently Okal (1977) has investigated the Rayleigh wave phase velocity, taking into account the lateral heterogeneities within oceanic plates.

This paper deals with regional differences in both phase velocity and Q of mantle

Rayleigh waves. Previous studies showed that Q of surface waves are strongly dependent on the paths but failed to find a regionality in Q. For example, Kanamori (1970a) states that the variation of Q appears to be almost unrelated to the tectonic nature of the path. One major reason for this failure of the previous studies may be their narrow path coverage.

5.2 CORRELATION BETWEEN THE MEASURED PHASE VELOCITY AND Q

Since the existence of a regionality in phase velocity has been relatively well established, we investigate a relation between the phase velocity and Q before the derivation of their pure-path values. Nakanishi (1978a, b) has discussed azimuthal variations of the phase velocity and Q. As this form of the display does not allow testing the hypothesis that the phase velocity and Q of Rayleigh waves have a close correlation with each other, using rigorous statistical method, we plot the observed phase velocity versus the observed Q^{-1} for a given period. Fig. 5 presents the phase velocity versus Q^{-1} plot at periods of 200 and 250 s. Although the scatter of the data points is considerable, it is clearly seen in the figure that the phase velocity has a negative correlation with Q^{-1}. We calculate the correlation coefficient between the phase velocity and Q^{-1} and test the statistical significance. The calculated correlation coefficients are plotted in Fig. 6. The absolute values of the correlation coefficients for 200 and 250 s are 0.254 and 0.271, respectively. We test the hypothesis:

$$\rho = 0, \tag{10}$$

where ρ is the correlation coefficient in the population. We calculated the correlation coefficients r_0 for the level of significance p with which the hypothesis (10) is rejected. r_0 equal 0.247 and 0.320 for $p = 0.05$ and 0.01, respectively. The comparison of these values of r_0 with the correlation coefficients at 200 and 250 s leads to the conclusion that we may reject the hypothesis (10) with the level of significance 0.05 and there is a correlation

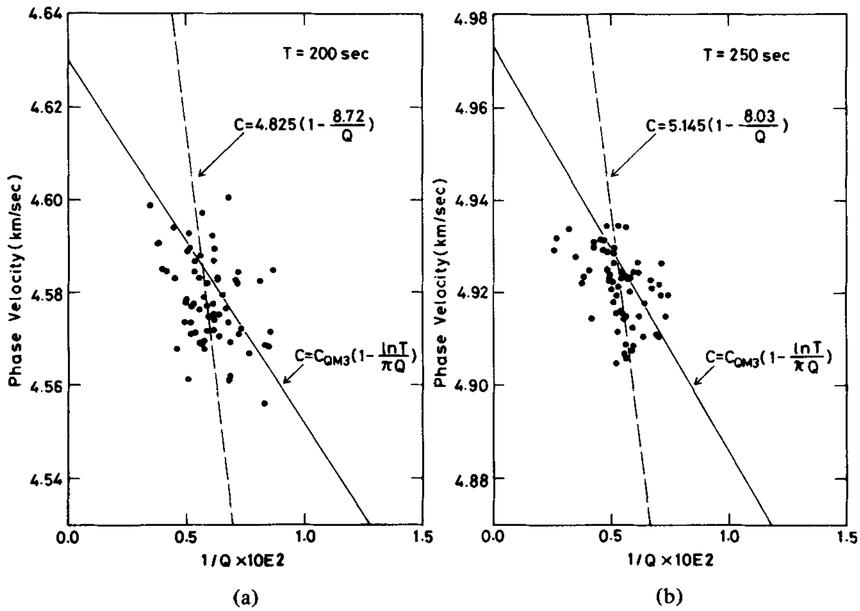

Figure 5. Phase velocity versus Q^{-1} plot. For explanation of the solid and dashed lines, see text. (a) 200 s, (b) 250 s.

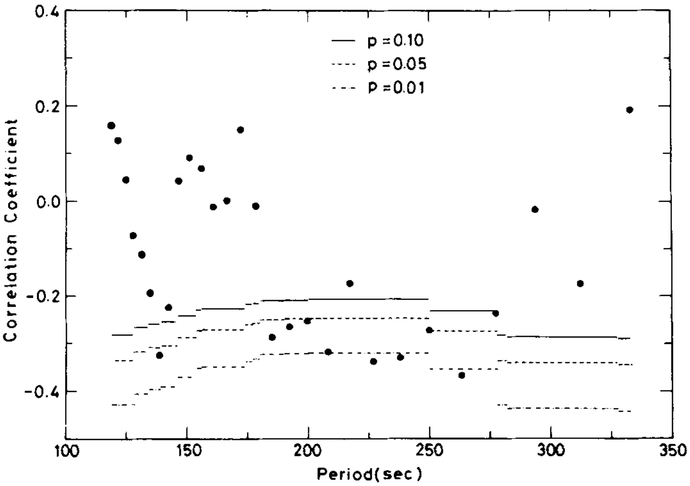

Figure 6. Correlation coefficients between phase velocity and Q^{-1} in the period range between 120 and 330 s. Solid, dashed and dot-dashed lines indicate the correlation coefficients for the level of significance p with which the hypothesis (10) (non-correlation) is rejected.

between the phase velocity and Q^{-1}. r_0 for $p = 0.1$, 0.05 and 0.01 are shown in Fig. 6. This figure indicates that there is a correlation between the phase velocity and Q^{-1} in the period range between 180 and 280 s.

Following Liu *et al.* (1976), the apparent phase velocity $C(T)$ of surface waves in an anelastic earth is expressed as

$$C(T) = C_0(T)\left[1 - \frac{\ln(T)}{\pi} \cdot \frac{1}{Q(T)}\right], \tag{11}$$

where $C_0(T)$ is the phase velocity for a 'one second' earth model and $Q(T)$ is the apparent quality factor of surface waves. If all the differences in phase velocities were related to variations in Q^{-1}, then all the points should fall on a straight line with the slope $-C_0(T)\cdot\ln(T)/\pi$. As the model QM3 of Hart (1977) represents a 'one second' earth model, we adopt the theoretical phase velocity for the model QM3 as $C_0(T)$ and obtain

$$C(T) = C_{QM3}(T)\left[1 - \frac{\ln(T)}{\pi} \cdot \frac{1}{Q}\right], \tag{12}$$

where $C_{QM3}(T)$ is the theoretical phase velocity for the model QM3. Equation (12) is shown in Fig. 5(a, b). The general trend of the data points is a little steeper than equation (12). Also shown in Fig. 5(a, b) are the least-squares fits to the data points. Here we assume that the phase velocity (ordinate) has no errors of measurement. Fig. 5(a, b) suggest that a large portion of the regional variations of phase velocity may be caused by the differences in Q^{-1}. We must collect much more data in order to answer the question, how large a portion of the differences in phase velocity is related to the variations in Q^{-1} and investigate the lateral variations in composition and state of the mantle of the Earth. The world-wide deployment of the ultra long-period seismometers (Agnew *et al.* 1976) will give an answer to this problem in the near future.

5.3 PURE-PATH PHASE VELOCITIES AND Q FOR FIVE TECTONIC PROVINCES

Since the regionality in phase velocity has been well established, the correlation between the phase velocity and Q^{-1} encourages us to attempt the inversion of pure-path Q of Rayleigh waves. Although Backus (1964) has formalized the inversion of lateral heterogeneities from surface waves, the path coverage of the present study is not dense enough, nor complete enough, to apply his theory to our data. Therefore, we investigate the lateral heterogeneities of the phase velocity and Q using the conventional pure-pathing method. We use Okal's (1977) regionalization scheme which is shown in Fig. 7. Okal divided the ocean into four different regions taking into account the lateral heterogeneities within the oceanic plates. We divided the ocean into two regions – oceanic and ridge – which are labelled O and R, respectively, in order to reduce the number of unknowns. O corresponds to 'A, B and C' of Okal and R is identical with his 'D'. We use the same regionalization and notation as Okal for shield (region S), mountainous region (region M), and trench and marginal sea (region T). Table 2 includes the percentages of path length, for each great-circle path, over regions S, M, T, R and O. The fractional path lengths were calculated by the intersection method on the computer. Nakanishi (1978a, b) indicates that the phase velocity and Q become lower in a systematic way as the 'mountainous' fraction increases. Fig. 8(a, b) shows a plot of the reciprocals of phase velocity and Q at 200 s versus 'mountainous' fraction. Although the scatter of the plots is considerable, these figures confirm our expectation that we will succeed in obtaining the pure-path phase velocity and Q. The observed phase velocity and Q are related to the pure-path phase velocity and Q for each region in the following manner,

$$\frac{l_S}{C_S(T)} + \frac{l_M}{C_M(T)} + \frac{l_T}{C_T(T)} + \frac{l_R}{C_R(T)} + \frac{l_O}{C_O(T)} = \frac{1}{C_{obs}(T)} \tag{13}$$

$$\frac{l_S}{Q_S(T)} + \frac{l_M}{Q_M(T)} + \frac{l_T}{Q_T(T)} + \frac{l_R}{Q_R(T)} + \frac{l_O}{Q_O(T)} = \frac{1}{Q_{obs}(T)} \tag{14}$$

for each period T, where C_S, C_M, C_T, C_R and C_O designate the pure-path phase velocity for regions S, M, T, R and O, Q_S, Q_M, Q_T, Q_R and Q_O are the pure-path Q for regions S, M, T,

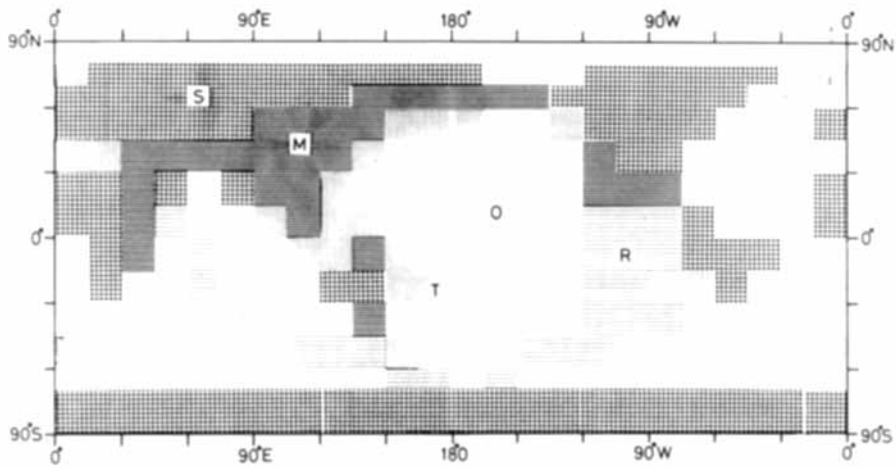

Figure 7. Okal's (1977) regionalization scheme used in the present study. S, shield; M, mountainous region; T, trench and marginal sea; R, ridge; O, oceanic region.

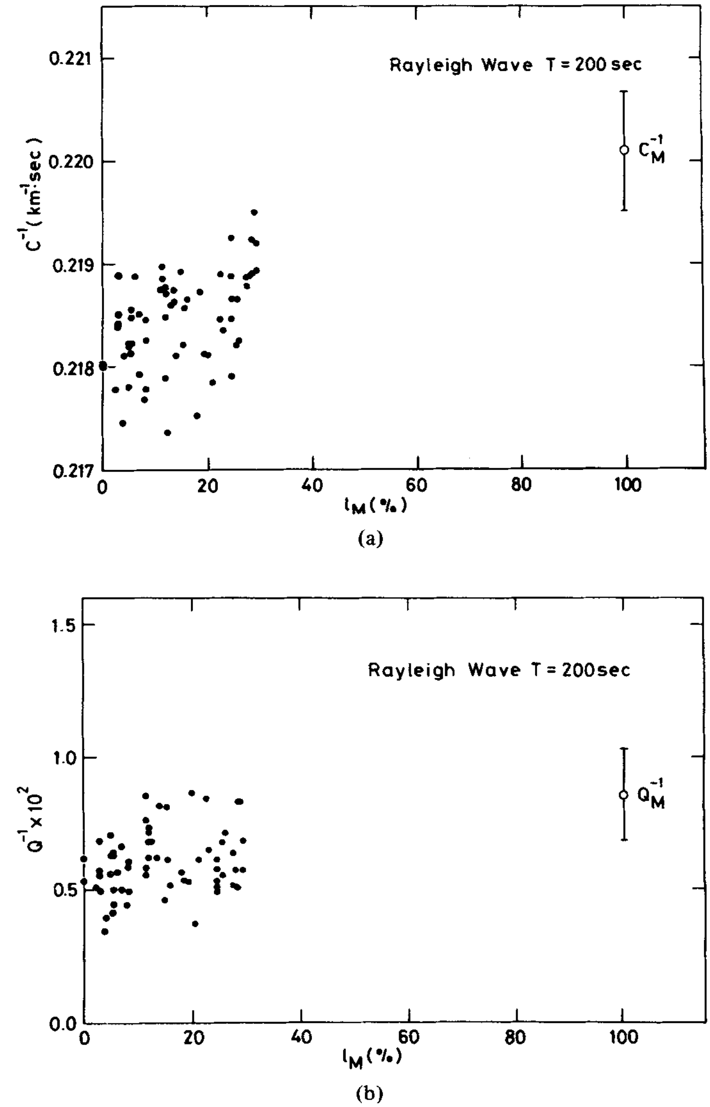

Figure 8. (a) Reciprocal of the phase velocity of Rayleigh waves versus l_M at 200 s. For explanation of C_M^{-1} and vertical bar, see text. (b) Q^{-1} of Rayleigh waves versus l_M at 200 s. For explanation of Q_M^{-1} and vertical bar, see text.

R and O, and C_{obs} and Q_{obs} represent the observed phase velocity and Q. We solve equations (13) and (14) using the least-squares technique. The results are given in Table 4(a) and Fig. 9(a) for phase velocity and in Table 4(b) and Fig. 9(b) for Q. The standard deviations are not shown in Fig. 9(a, b) in order to avoid the confusion in the figures. The results in the period range between 200 and 300 s, where the quality of the data is best, are as follows: the 'shield' has the highest phase velocity and Q, the 'mountainous' region has the lowest phase velocity and Q, and the 'trench and marginal sea' and 'ridge' regions have the intermediate phase velocities and the lowest Q. However, the standard deviations for 'trench and marginal sea' and 'ridge' regions are large. C_O and Q_O are the most certain because of the

Table 4. (a) Pure-path phase velocities and their standard deviations of Rayleigh waves for five regions. (b) Pure-path Q and their standard deviations of Rayleigh waves for five regions.

(a)

T sec	C_S km/sec	σC_S km/sec	C_M km/sec	σC_M km/sec	C_T km/sec	σC_T km/sec	C_R km/sec	σC_R km/sec	C_O km/sec	σC_O km/sec
294.12	5.2752	0.0190	5.2426	0.0142	5.2614	0.0319	5.2343	0.0291	5.2440	0.0139
277.78	5.1521	0.0131	5.1141	0.0107	5.1408	0.0186	5.1209	0.0129	5.1230	0.0078
263.16	5.0430	0.0142	4.9948	0.0115	5.0234	0.0200	5.0241	0.0139	5.0185	0.0084
250.00	4.9467	0.0134	4.8872	0.0107	4.9139	0.0190	4.9330	0.0145	4.9240	0.0076
238.10	4.8556	0.0147	4.7957	0.0116	4.8231	0.0206	4.8405	0.0158	4.8401	0.0083
227.27	4.7775	0.0159	4.7217	0.0127	4.7525	0.0225	4.7567	0.0170	4.7692	0.0090
217.39	4.7076	0.0144	4.6548	0.0116	4.6817	0.0206	4.6777	0.0154	4.7031	0.0082
208.33	4.6489	0.0151	4.5967	0.0120	4.6197	0.0211	4.6136	0.0161	4.6476	0.0086
200.00	4.5942	0.0150	4.5386	0.0120	4.5566	0.0211	4.5554	0.0159	4.5949	0.0085
192.31	4.5450	0.0150	4.4922	0.0119	4.5119	0.0212	4.5039	0.0162	4.5505	0.0085
185.19	4.5030	0.0158	4.4461	0.0127	4.4683	0.0224	4.4660	0.0174	4.5110	0.0090
178.57	4.4709	0.0182	4.4064	0.0154	4.4222	0.0258	4.4360	0.0206	4.4721	0.0105
172.41	4.4383	0.0182	4.3750	0.0159	4.3758	0.0258	4.4003	0.0200	4.4362	0.0096
166.67	4.4143	0.0226	4.3544	0.0198	4.3360	0.0318	4.3656	0.0246	4.4108	0.0120
161.29	4.3834	0.0279	4.3313	0.0246	4.2978	0.0394	4.3214	0.0302	4.3856	0.0149
156.25	4.3632	0.0304	4.3183	0.0266	4.2674	0.0422	4.2856	0.0328	4.3711	0.0162
151.52	4.3426	0.0296	4.2981	0.0268	4.2293	0.0403	4.2507	0.0328	4.3490	0.0159
147.06	4.3207	0.0380	4.2867	0.0347	4.2015	0.0524	4.2148	0.0422	4.3324	0.0194
142.86	4.3088	0.0461	4.2673	0.0440	4.1742	0.0589	4.1907	0.0535	4.3155	0.0238
138.89	4.3030	0.0464	4.2389	0.0437	4.1407	0.0584	4.1789	0.0534	4.2999	0.0238
135.14	4.3081	0.0465	4.2019	0.0425	4.0992	0.0570	4.1806	0.0535	4.2843	0.0237
131.58	4.3093	0.0459	4.1692	0.0403	4.0579	0.0537	4.1808	0.0514	4.2677	0.0225
128.21	4.2999	0.0495	4.1491	0.0436	4.0250	0.0561	4.1737	0.0594	4.2544	0.0240
125.00	4.2836	0.0602	4.1417	0.0551	3.9999	0.0674	4.1593	0.0878	4.2473	0.0307
121.95	4.2470	0.0700	4.1444	0.0650	3.9999	0.0784	4.1272	0.1019	4.2406	0.0362
119.05	4.2011	0.0825	4.1552	0.0768	4.0285	0.0911	4.0869	0.1193	4.2326	0.0429

(b)

T sec	Q_S	σQ_S	Q_M	σQ_M	Q_T	σQ_T	Q_R	σQ_R	Q_O	σQ_O
294.12			159	90	74	47	87	44	245	153
277.78	629	224	173	63	101	41	96	19	264	110
263.16	348	298	165	43	119	42	107	22	273	74
250.00	300	84	149	31	121	39	117	23	255	70
238.10	286	111	135	24	115	32	126	30	240	61
227.27	293	187	126	23	112	30	133	38	225	51
217.39	294	204	122	22	116	33	133	37	211	44
208.33	254	124	120	22	131	44	131	32	197	44
200.00	205	87	118	24	153	77	129	37	182	41
192.31	159	77	121	26	196	109	120	53	168	36
185.19	122	41	135	37	262	322	102	31	161	36
178.57									159	43
172.41									157	38
166.67									153	42
161.29									144	44
156.25									132	37
151.52									124	32
147.06									125	27
142.86									132	43
138.89									148	57
135.14									157	66
131.58									158	79
128.21									153	83
125.00									154	82
121.95									173	115
119.05									201	174

large path fraction over 'oceanic' regions. The difference between C_S and C_O or Q_S and Q_O is relatively small considering their standard deviations. The difference between C_M and C_S or C_O is significant. The same result is obtained for Q. These results quantitatively confirm the regional differences in phase velocity and Q described by Nakanishi (1978b) in qualitative manner. Since we used the same regionalization scheme as Okal (1977), we compare our results with those of Okal. The comparison is made in Fig. 9(a, c). C_S and C_T obtained in the present study are different from those obtained by Okal. Our C_S corresponds to the theoretical phase velocity calculated by Okal for the oldest region of the ocean (Kausel, Leeds & Knopoff 1974; Leeds, Kausel & Knopoff 1974; Leeds 1975; Yoshii 1975). The present study supports Okal's conclusion that the phase velocities for 'shield' and 'mountainous' regions are substantially different from the mean oceanic ones, but they still

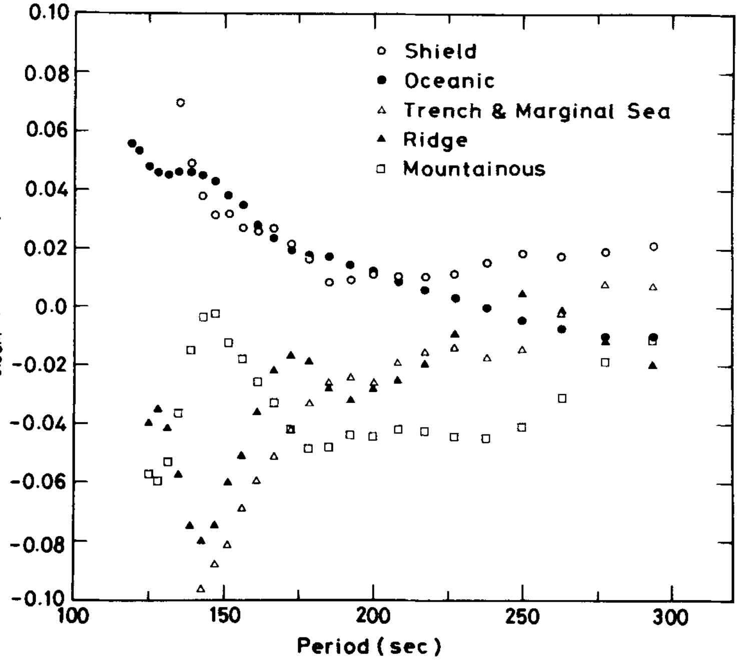

(a)

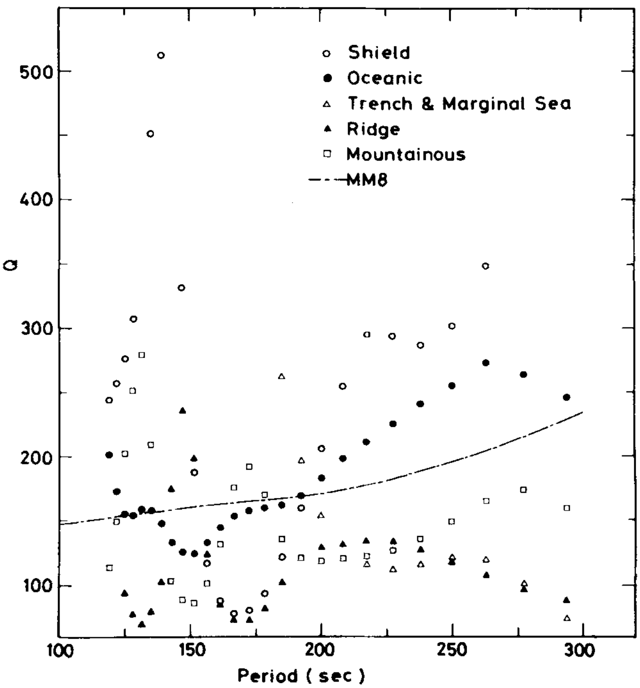

(b)

Figure 9. Results of pure-pathing analysis. (a) Pure-path phase velocities of Rayleigh waves for five regions. (b) Pure-path Q of Rayleigh waves for five regions. (c) Okal's (1977) pure-path phase velocities of Rayleigh waves for three regions.

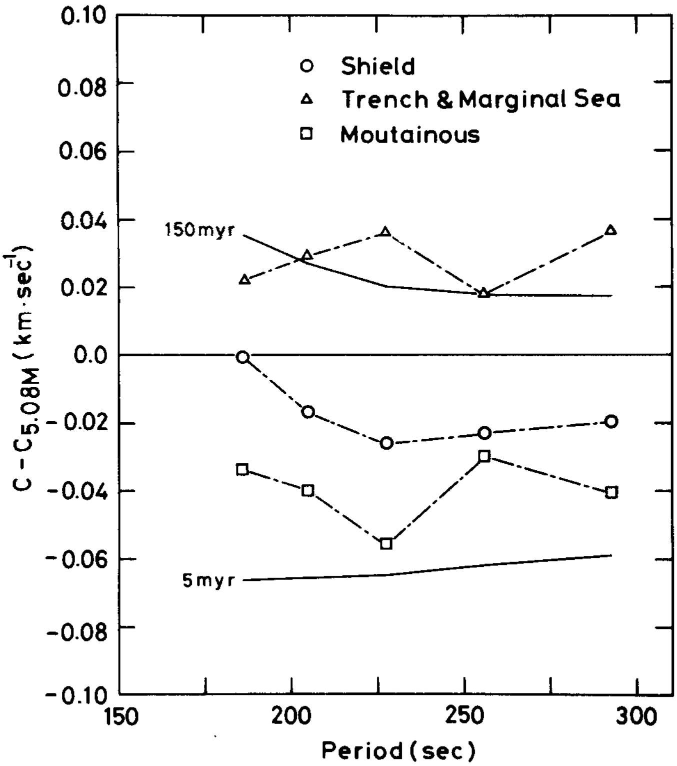

Figure 9 (c)

fall within the range of variation of oceanic phase velocities with age of plate. It is worth noting that the continent may be divided into such distinct regions as 'shield' and 'mountainous'. This result suggests that we have to pay more attention to the subdivision within the continent in order to improve our understanding of the lateral heterogeneities in the deep mantle. We will present the regionalized shear wave velocity and Q structures inverted from the results of the present study in a separate paper.

6 Discussion

In the previous section we have found that Rayleigh waves suffer small attenuation along the path where the observed phase velocity is high and large attenuation over the region where the observed phase velocity is low. This correlation between the phase velocity and Q is seemingly reasonable but some caution is required to interpret it. Following Liu *et al.* (1976), we need to correct the observed phase velocity by the formula:

$$\Delta C(T) = \frac{C(T)}{\pi \cdot Q(T)} \ln(T), \tag{15}$$

where T is the period, $C(T)$ the observed phase velocity and $Q(T)$ the observed quality factor. The reference period is chosen here to be equal to 1 s which is the characteristic period of body wave studies. This correction provides the phase velocity data from which the 'one second' upper mantle model can be derived and is required to perform the joint inversion of body wave and surface wave data. Equation (15) and the correlation between

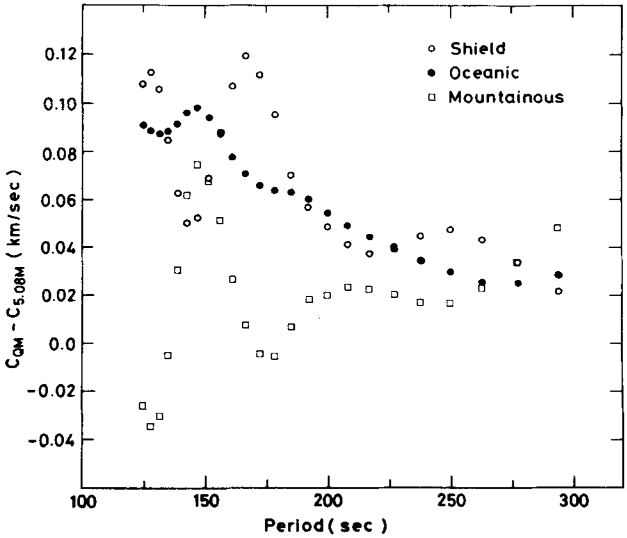

Figure 10. Q-corrected pure-path phase velocities of Rayleigh waves for shield, oceanic and mountainous regions. C_{QM} indicates the pure-path phase velocity corrected for attenuation using the pure-path Q.

the observed phase velocity and Q lead to an important conclusion that the lateral heterogeneities in the 'one second' earth are much smaller than those derived from the apparent phase velocities without Q-correction. We correct the pure-path phase velocities using the pure-path Q values. The corrected pure-path phase velocities for 'shield', 'mountainous' and 'oceanic' regions are shown in Fig. 10. It is seen in the figure that the difference between C_M and either C_S or C_O is considerably reduced and the difference is only 0.025 km/s, 50 per cent of the difference for the uncorrected phase velocities, in the period range between 200 and 300 s. This result indicates that currently expected lateral heterogeneities may be overestimated and that all the previous investigations on lateral heterogeneities using surface waves are incomplete in principle. The corrected C_T and C_R have the highest values which are due to the lowest Q for the 'trench and marginal sea' and 'ridge' regions. The standard deviations of phase velocities and Q for these regions are very large because of the short fractional path lengths. The above discussion, however, does not necessarily mean the absence of a significant regional difference in the observed phase velocities. Frequency-independent Q, which is the basic assumption of equation (15), may not be valid for the seismic wave attenuation processes operating in the upper mantle of the Earth. Several authors (Archambeau, Flinn & Lambert 1969; Tsai & Aki 1969; Solomon 1972; Yoshida & Tsujiura 1975 and Der & McElfresh 1977), for example, report frequency-dependent Q. Broad-band observations of body waves are required to exploit the frequency-dependence of Q and then to make the appropriate correction to the observed phase velocities.

7 Conclusions

The following conclusions may be drawn from the present analysis.

(1) Rayleigh waves suffer small attenuation along the path where the observed phase velocity is high and large attenuation over the region where the observed phase velocity is low. This correlation is significant in the statistical sense in the period range between 180

and 280 s. This result indicates that the lateral heterogeneities may be much smaller than those derived from the observed phase velocities without correction for attenuation.

(2) The regional differences exist in both the phase velocity and Q of Rayleigh waves. The quality factor Q for such tectonically active regions as 'mountainous', 'trench and marginal sea' and 'ridge' have a value of about 130 throughout the period range between 200 and 300 s.

(3) Although Q of the model MM8 (Anderson *et al.* 1965) is appropriate as an average representation of the observed Q in the period range from 200 to 300 s, the differences for different great-circle paths are very large.

(4) The low-Q zone in the upper mantle must be more extensive than that of model MM8.

Acknowledgments

I am grateful to Dr Yoshio Fukao for making valuable suggestions. I thank Professor Tokuji Utsu for kindly reading the manuscript, and Professor Masanori Saito for sending me the unpublished notes and the program of Wiener filtering and for reading the manuscript. I thank Drs F. Wu and J. Dewey for reviewing the paper and offering valuable suggestions. I benefited from the valuable criticisms and suggestions of Dr A. Dziewonski. Following his suggestions the early draft of this paper was improved.

References

Abe, K., Sato, Y. & Frez, J., 1970. Free oscillations of the Earth excited by the Kurile Islands earthquake 1963, *Bull. Earthq. Res. Inst.*, **48**, 87–114.

Agnew, D., Berger, J., Buland, R., Farrell, W. & Gilbert, F., 1976. International deployment of accelerometers: a network for very long period seismology, *EOS, Trans. Am. geophys. Un.*, **57**, 180–188.

Akopyan, S. Ts., Zharkov, V. N. & Lyubimov, V. M., 1975. The dynamic shear modulus in the interior of the Earth, *Dokl. Akad. Nauk SSSR, Earth Sci. Sections*, **223**, 1–3.

Akopyan, S. Ts., Zharkov, V. N. & Lyubimov, V. M., 1976. Corrections to the eigenfrequencies of the Earth due to dynamic shear modulus, *Izv. Akad. Nauk SSSR, Phys. solid Earth*, **12**, 625–630.

Anderson, D. L., Ben-Menahem, A. & Archambeau, C. B., 1965. Attenuation of seismic energy in the upper mantle, *J. geophys. Res.*, **70**, 1441–1448.

Archambeau, C. B., Flinn, E. A. & Lambert, D. G., 1969. Fine structure of the upper mantle, *J. geophys. Res.*, **67**, 282–289.

Backus, G. E., 1964. Geographical interpretation of measurements of average phase velocities of surface waves over great circular and great semicircular paths, *Bull. seism. Soc. Am.*, **54**, 571–610.

Ben-Menahem, A., 1965. Observed attenuation and Q values of seismic surface waves in the upper mantle, *J. geophys. Res.*, **70**, 4641–4651.

Cara, M., 1973. Filtering of dispersed wave-trains, *Geophys. J. R. astr. Soc.*, **33**, 65–80.

Carpenter, E. W. & Davies, D., 1966. Frequency dependent seismic phase velocities, an attempted reconciliation between the Jeffreys/Bullen and the Gutenberg models of the upper mantle, *Nature*, **212**, 134–135.

Claerbout, J. F. & Robinson, E. A., 1964. The error in least squares inverse filtering, *Geophysics*, **29**, 118–120.

Dahlen, F. A., 1975. The correction of great-circular surface wave phase velocity measurements for the rotation and ellipticity of the Earth, *J. geophys. Res.*, **80**, 4895–4903.

Dahlen, F. A., 1976. Reply (to Dziewonski and Sailor), *J. geophys. Res.*, **81**, 4951.

Der, Z. A. & McElfresh, T. W., 1977. The relation between anelastic attenuation and regional amplitude anomalies of short-period P waves in North America, *Bull. seism. Soc. Am.*, **67**, 1303–1317.

Deschamps, A., 1977. Inversion of the attenuation data of free oscillations of the Earth (fundamental and first higher modes), *Geophys. J. R. astr. Soc.*, **50**, 699–722.

Dziewonski, A. M., 1971a. On regional differences in dispersion of mantle Rayleigh waves, *Geophys. J. R. astr. Soc.*, **22**, 289–325.

Dziewonski, A. M., 1971b. Upper mantle models from 'pure-path' dispersion data, *J. geophys. Res.*, **76**, 2587–2601.

Dziewonski, A. M., Bloch, S. & Landisman, M., 1969. A technique for the analysis of transient seismic signals, *Bull. seism. Soc. Am.*, **59**, 427–444.

Dziewonski, A. M. & Gilbert, F., 1972. Observations of normal modes from 84 recordings of the Alaskan earthquake of 1964 March 28, *Geophys. J. R. astr. Soc.*, **27**, 393–446.

Dziewonski, A. M., Mills, J. & Bloch, S., 1972. Residual dispersion measurements – a new method of surface wave analysis, *Bull. seism. Soc. Am.*, **62**, 125–135.

Dziewonski, A. M. & Sailor, R. V., 1976. On the effect of the Earth's ellipticity on velocity of mantle waves, *J. geophys. Res.*, **81**, 4947–4950.

Futterman, W. I., 1962. Dispersive body waves, *J. geophys. Res.*, **67**, 5279–5291.

Hart, R. S., 1977. The distribution of seismic velocities and attenuation in the Earth, *PhD thesis*, California Institute of Technology, Pasadena.

Jackson, D. D. & Anderson, D. L., 1970. Physical mechanisms of seismic-wave attenuation, *Rev. Geophys. Space Phys.*, **8**, 1–63.

Jeffreys, H., 1965. Damping of *S* waves, *Nature*, **208**, 675.

Jeffreys, H., 1975. Importance of damping in geophysics, *Geophys. J. R. astr. Soc.*, **40**, 23–27.

Jobert, N. & Roult, G., 1976. Periods and damping of free oscillations observed in France after sixteen earthquakes, *Geophys. J. R. astr. Soc.*, **45**, 155–176.

Kanamori, H., 1970a. Velocity and Q of mantle waves, *Phys. Earth planet. Int.*, **2**, 259–275.

Kanamori, H., 1970b. Synthesis of long-period surface waves and its application to earthquake source studies – Kurile Islands earthquake of October 13, 1963, *J. geophys. Res.*, **75**, 5011–5027.

Kanamori, H., 1970c. The Alaska earthquake of 1964: Radiation of long-period surface waves and source mechanism, *J. geophys. Res.*, **75**, 5029–5040.

Kanamori, H., 1971. Focal mechanism of the Tokachi-oki earthquake of May 16, 1968: Contortion of the lithosphere at a junction of two trenches, *Tectonophys.*, **12**, 1–13.

Kanamori, H. & Anderson, D. L., 1977. Importance of physical dispersion in surface wave and free oscillation problems: Review, *Rev. Geophys. Space Phys.*, **15**, 105–112.

Kausel, E. G., Leeds, A. R. & Knopoff, L., 1974. Variations of Rayleigh wave phase velocity across the Pacific Ocean, *Science*, **186**, 139–141.

Kikuchi, M., 1977. An estimation method of impulse response and its application (in Japanese), *Zisin*, **30**, 265–273.

Leeds, A. R., 1975. Lithospheric thickness in the Western Pacific, *Phys. Earth planet. Int.*, **11**, 61–64.

Leeds, A. R., Kausel, E. G. & Knopoff, L., 1974. Variations of upper mantle structure under the Pacific Ocean, *Science*, **186**, 141–143.

Levinson, N., 1947. The Wiener rms (root mean square) error criterion in filter design and prediction, *J. Math. Phys.*, **25**, 261–278.

Liu, H. P., Anderson, D. L. & Kanamori, H., 1976. Velocity dispersion due to anelasticity; implication for seismology and mantle composition, *Geophys. J. R. astr. Soc.*, **47**, 41–58.

Luh, P. C., 1974. Normal modes of a rotating, self-gravitating inhomogeneous Earth, *Geophys. J. R. astr. Soc.*, **38**, 187–224.

Maruyama, T., 1967. On the geodesic once around the geoellipsoid (in Japanese), *Zisin*, **20**, 50–53.

Mills, J. M. & Hales, A. L., 1977. Great-circle Rayleigh wave attenuation and group velocity, Part I: Observations for periods between 150 and 600 seconds for seven great-circle paths, *Phys. Earth planet. Int.*, **14**, 109–119.

Nakanishi, I., 1978a. Measurements of phase velocity and Q of mantle Rayleigh waves, *Master thesis*, Nagoya University, Nagoya.

Nakanishi, I., 1978b. Regional differences in the phase velocity and the quality factor Q of mantle Rayleigh waves, *Science*, **200**, 1379–1381.

Okal, E. A., 1977. The effect of intrinsic oceanic upper-mantle heterogeneities on regionalization of long-period Rayleigh-wave phase velocities, *Geophys. J. R. astr. Soc.*, **49**, 357–370.

Payo, G., 1969. Atenuacion de ondas sismicas, *Rev. Geofis.*, **28**, 277–315.

Pennington, R. H., 1965. *Introductory Computer Methods and Numerical Analysis*, The Macmillan Company, New York.

Randall, M. J., 1976. Attenuative dispersion and frequency shifts of the Earth's free oscillations, *Phys. Earth planet. Int.*, **12**, P1–P4.

Reiter, L., 1973. Reflection, refraction and mode conversion of long-period surface waves and the measurement of Q^{-1} for free oscillations, *Bull. seism. Soc. Am.*, **63**, 1709–1722.

Robinson, E. A. & Treitel, S., 1967. Principles of digital Wiener filtering, *Geophys. Prosp.*, **15**, 311–333.

Roult, G., 1974. Atténuation des ondes seismiques de très basse fréquence, *Ann. Géophys.*, **30**, 141–167.

Roult, G., 1975. Attenuation of seismic waves of very low frequency, *Phys. Earth planet. Int.*, **10**, 159–166.

Sailor, R. V. & Dziewonski, A. M., 1978. Measurements and interpretation of normal mode attenuation, *Geophys. J. R. astr. Soc.*, **53**, 559–581.

Saito, M., 1976. Estimation of spectral ratio by Wiener filter (in Japanese), *Abstract for Ann. Meet. Seismol. Soc. Japan.*

Smith, S. W., 1972. The anelasticity of the mantle, *Tectonophys.*, **13**, 601–622.

Solomon, S. C., 1972. On Q and seismic discrimination, *Geophys. J. R. astr. Soc.*, **31**, 163–177.

Toksöz, M. N. & Anderson, D. L., 1966. Phase velocities of long-period surface waves and structure of the upper mantle. I. Great-circle Love and Rayleigh wave data, *J. geophys. Res.*, **73**, 3801–3806.

Tsai, Yi-Ben & Aki, K., 1969. Simultaneous determination of the seismic moment and attenuation of seismic surface waves, *Bull. seism. Soc. Am.*, **59**, 275–287.

Umbgrove, J. H. F., 1947. *The Pulse of the Earth*, 2nd edn, Nijhoff, The Hague.

Wiener, N., 1949. *Extrapolation, Interpolation and Smoothing of Stationary Time Series*, The MIT Press.

Wiggins, R. A. & Robinson, E. A., 1965. Recursive solution to the multichannel filtering problem, *J. geophys. Res.*, **70**, 1885–1891.

Wu, F. T., 1972. Mantle Rayleigh wave dispersion and tectonic provinces, *J. geophys. Res.*, **77**, 6445–6453.

Wu, F. T. & Kanamori, H., 1973. Source mechanism of Feb. 4, 1965, Rat Island earthquake, *J. geophys. Res.*, **78**, 6082–6091.

Yoshida, M. & Tsujiura, M., 1975. Spectrum and attenuation of multiply reflected core phases, *J. Phys. Earth*, **23**, 31–42.

Yoshii, T., 1975. Regionality of group velocities of Rayleigh waves in the Pacific and thickening of the plate, *Earth planet. Sci. Lett.*, **25**, 305–312.